J Solid State Electrochem (2007) 11: 273–282
DOI 10.1007/s10008-006-0104-4

ORIGINAL PAPER

M. Yousef Elahi · H. Heli · S. Z. Bathaie · M. F. Mousavi

Electrocatalytic oxidation of glucose at a Ni-curcumin modified glassy carbon electrode

Received: 7 July 2005 / Accepted: 23 January 2006 / Published online: 27 April 2006

Abstract The electrocatalytic oxidation of glucose was investigated on a nickel-basedchemically modified electrode (Ni(II)-curcumin) prepared by electropolymerization of Ni-curcumin complex (curcumin=1,7-bis[4-hydroxy-3-methoxyphenyl]-1,6-heptadiene-3,5-dione) in alkaline solution. Reaction kinetic and mechanism were investigated by using cyclic voltammetry (CV) and chronoamperometry (CA) techniques and steady-state polarization measurements. Cyclic voltammetry studies indicated that in the presence of glucose the anodic peak current of surface redox mediator was increased, followed by decrease in the corresponding cathodic current. This indicates that glucose was oxidized at the surface of this modified electrode. The results were explained based on the concept of electrocatalytic reactions that occur in this chemically modified electrode. The diffusion coefficient of glucose and the rate constant of the catalytic oxidation of glucose were found to be 6.7×10^{-6} cm^2 s^{-1} and 6.5×10^{3} M^{-1} s^{-1}, respectively. It has shown that by using the Ni-curcumin modified electrode, glucose can be determined with good response and low detection limit.

Keywords Nickel · Curcumin · Glucose · Modified electrode · Electrocatalysis

Introduction

Chemically modified electrodes (CMEs) have attracted much interest in the study of the electrocatalytic oxidation/reduction of important redox systems. Modified electrodes can be prepared by deposition of various compounds such as organic compounds, conducting polymers, add-atoms of metals, etc. on the various electrodes. In the recent years, electrodes coated with metallated electroactive polymers have received increased attention [1–3]. They are widely characterized used for the electrooxidation of several organic substrates [4]. Indeed, recent researches in developing new electrode materials seem to be directed towards the use of macrocyclic complexes in the form of conducting polymer films [5] that behave as fast electron transfer mediators for solution species. Although electrochemistry and electrocatalytic properties of macrocyclic complexes of some transition metals have been well studied in various solvents [6], few data about their behavior as electropolymerized films in aqueous alkaline solution exist. Recently, it has been shown that nickel macrocyclic complexes can be easily electropolymerized onto an electrode surface in alkaline solution to form modified electrodes that catalyzed oxidation of several substrates [7–9]. The most utilized electrode for electrooxidation and determination of carbohydrates has been those that contained Ni (II)/Ni (III) redox couple which can improve the sensitivity for the determination of carbohydrates [10]. Chemically modified electrodes with nickel compounds were developed by depositing Ni or its complexes on a traditional electrode surface (Au, carbon, diamond) via chemical, electrochemical, or physical routes [11]. Determination and measurement of carbohydrates have considerable importance in food industry, biotechnology, environmental, and clinical diagnostics [12].

Recently electrooxidation of glucose and some other monosaccharides were studied on various metals such as platinum [13], copper [14], and gold [15] and also on modified surfaces such as ruthenium dioxide [16], nickel oxide [17], and metallic complexes such as cobalt phthalocyanine [18]. Also, it is well known that the kinetics of the glucose oxidation reaction is affected by the type of electrode materials and the metallated electroactive polymers [19]. Alternatively, Ojani et al. [20] have reported on the use of a poly(1-naphttylamine)/nickel-modified

M. Yousef Elahi · H. Heli · M. F. Mousavi (✉)
Department of Chemistry, Faculty of Science,
Tarbiat Modarres University,
P. O. Box 14115-175 Tehran, Iran
e-mail: mousavim@modares.ac.ir
Tel.: +98-21-88011001
Fax: +98-21-88006544

S. Z. Bathaie
Department of Clinical Biochemistry,
Faculty of Medical Science, Tarbiat Modarres University,
Tehran, Iran

carbon paste electrode for detection of some carbohydrates. A recent work by Warren et al. [21] has shown that metal picolinate complexes were evaluated as mediators for a glucose oxidase based biosensor, and Araki et al. [22] have reported a new glucose sensor, based on the electropolymerization of the supramolecular species tetra{bis(2,2_-bipyridyl)chlororuthenium(II)}.

As a follow-up of our recent studies of the electrocatalysis and electrooxidation of some compounds [23, 24], the electrocatalytic oxidation of glucose on Ni-curcumin-modified glassy carbon electrode (NCGC) in alkaline medium is described in this work.

Materials and methods

Chemicals and instrumentation

Sodium hydroxide, nickel chloride, ammonia solution, curcumin (1,7-bis[4-hydroxy-3-methoxyphenyl]-1,6-heptadiene-3,5,dione), and glucose used in this work were prepared from Merck as analytical reagent grade chemicals. The Ni(II)-ammonia complex was synthesized. Electrochemical studies were carried out in a conventional threes electrode cell powered by an Autolab PGSTAT30 potentiostat/galvanostat (Eco Chemie, Utrecht, The Netherlands). A glassy carbon electrode (GC, Metrohm, modified or else), an Ag/AgCl sat'd KCl, and a Pt wire was used as working reference and counter electrodes, respectively. All studies were carried out at room temperature.

Modification of the working electrode

The GC electrode polished on a polishing microcloth with 0.05 μm alumina powder and rinsed thoroughly with distilled deionized water before modification. The electrode was placed in 0.1 M NaOH containing 10 mM curcumin and 4 mM Ni(II)-ammonia complex subsequent by applying the potential between 200 and 800 mV at a scan rate of 100 mV s^{-1} in a cyclic voltammetry regime. For preparation of $[Ni(NH_3)_4]^{2+}$ complex, $NiCl_2$ (4 mM) was dissolved in 25% ammonia solution [NH_3 as complexion agent of Ni(II) ion]. Experiment is performed in a solution containing an excess amount of curcumin for completion of the reaction of Ni-curcumin complex formation.

Results and discussion

Figure 1 represents 40 consecutive cyclic voltammograms of 0.1 M NaOH solution containing 10 mM curcumin and 4 Mm Ni(II)-ammonia complex and shows the evolution of the cyclic voltammogram obtained for Ni-curcumin film growth, denoted poly Ni-curcumin, on a glassy carbon electrode. The potential was continuously cycled between 200 and 800 mV and the potential sweep rate of 100 mV s^{-1} was used. The continuous increase in the amplitude of the voltammometric peaks indicates that the film is formed as a result of the anodic electropolymerization of the curcumin complex.

Another point in Fig. 1 is the appearance of a pair of oxidation/reduction peaks around 580 and 440 mV, respectively. These well-defined peaks were attributed to the formation and immobilization of polyNi-curcumin film on the electrode surface [9]. The redox reaction that occur

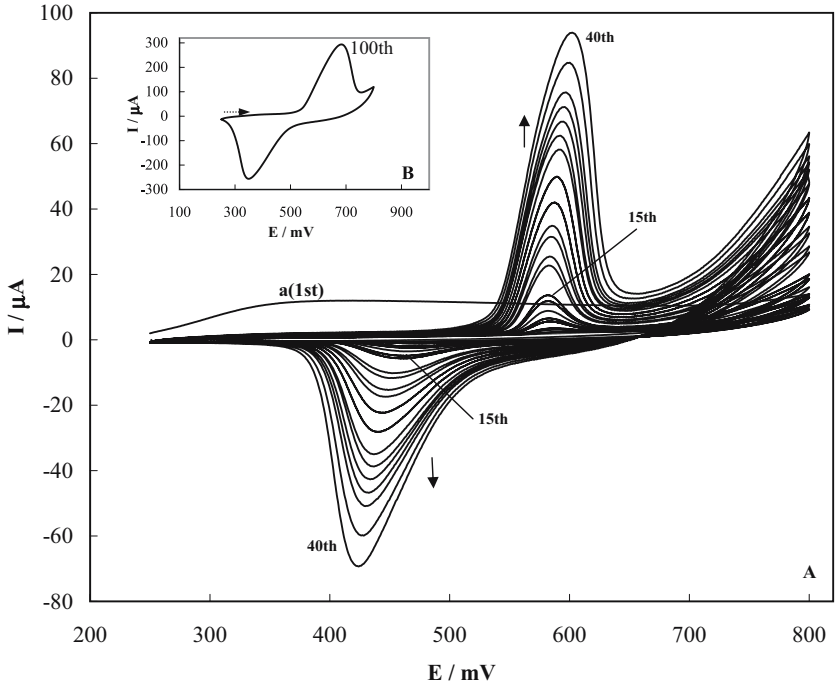

Fig. 1 **a** Consequtive cyclic voltammograms of 0.1 M NaOH solution containing Ni(II)-curcumin complex using a GC electrode with scan rate of 100 mV s^{-1}. Curve *a* is the first cycle due to oxidation of curcumin. **b** Cyclic voltammogram of 0.1 M NaOH solution containing Ni(II)-curcumin complex using a GC electrode after applying 100 potential cycles

during anodic/cathodic cycle is related to the Ni(II)-curcumin/Ni (III)-curcumin transition. Film formation on the surface was further confirmed by applying 100 cycles of potential in the solution containing Ni-curcumin complex. Based on previously reported works [9], the 100 cycles was selected as the optimum value for further studies. After a period of scanning, the electrode was transferred, after careful rinsing with distilled water, to a 0.1 M NaOH aqueous solution (containing no monomer). The cyclic voltammogram of the poly NCGC film is shown in Fig. 1; inset exhibits the previously observed electrochemical behavior assigned to the Ni(II)-Ni(III) process [25]. The oxidation/reduction peaks that appeared did not change upon further potential cycling.

On the first cycle, a well-defined irreversible anodic peak appears at a potential about 350 mV. This signal is due to adsorption of curcumin and its oxidation on the electrode surface. In addition, this peak disappeared in the next scan and the presumed Ni(II)/Ni(III) redox system was clearly evident by the second scan and no anodic peak appeared around 350 mV. Such behavior is indicated by rapid deposition of a nonconducting polymer on the electrode surface. The difference between the first voltammogram and subsequent scans has also been reported in the studies of the oxidative electropolymerization of other Ni(II) complexes [26–28].

Curcumin as an antioxident and as a scavenger of reactive oxygen species [29] has a unique conjugated structure including two methoxylated phenols and an enol form of â-diketone (Fig. 2a). According to the reduction potentials of the corresponding orthophenoxyl radicals [30], two orthomethoxyphenols in curcumin can be very moderate electron donors. Additionally, it is well known that phenols in strong alkaline solutions exist as a corresponding phenolate ion **I**, which is readily oxidize via one electron transfer process and followed by generating free radicals **II**. The presence of the methoxy group in the monomer makes many follow-up reactions possible. First, by alkaline hydrolysis, the methanol molecule can be eliminated from radical **II** giving an anion radical **III**, which, via the other one-electron reaction, is converted to a highly reactive *o*-quinone **IV**. Figure 2c presents the main possible reactions involved in the electrooxidation of the curcumin molecule. It could be expected that the quinone **IV** derived from *o*-methoxyphenol substrate would be reduced reversibly during contin-

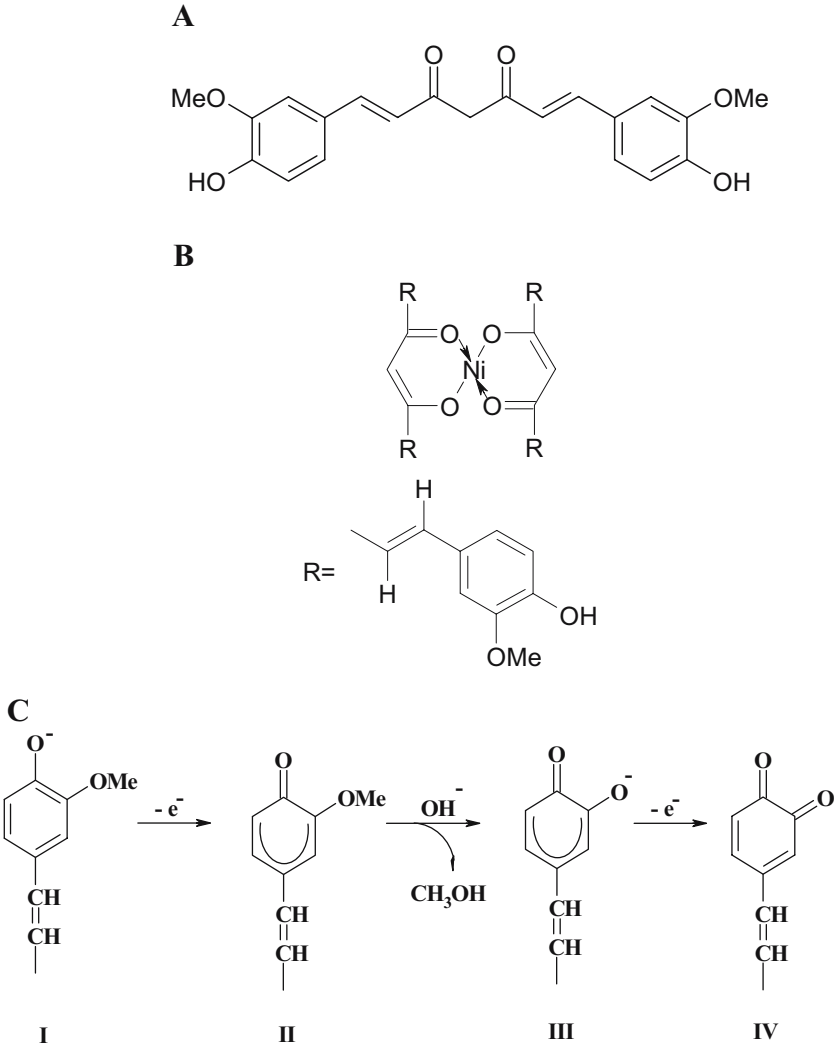

Fig. 2 **a** The chemical structure of curcumin. **b** The chemical structure of Ni(II)-curcumin complex. **c** Possible reaction routes involved into electropolymerization of curcumin ligand

uous potential cycling to the corresponding hydroquinone, giving rise to a characteristic redox couple [31]. In practice, it is seldom observed.

Possible mechanisms to account for the creation of the polymer matter on electrode may include the following steps: (1) a free radical step-growth polymerization initiated by **II** as suggested for a mixture of phenol and 4-allylphenol leading to a poly(oxyphenylene) film [32], (2) Diels-Alder reaction between *o*-quinone **IV** and allyl C=C bound giving a 1,4-benzenedioxane subunit, (3) dimerization of the radical **II**, (4) creation of lignan-like subunits by oxidative coupling of the substrate molecules [33], and (5) hydroxylation of the *o*-quinone IV leading to the corresponding *p*-quinone [34]. Consequently, a poorly defined, highly cross-linked, compact structure is formed on the electrode surface.

The electron-donating ability of curcumin is assessed from the measurements of one-electron-transfer equilibria of dehydrozingerone (DHZ) radicals [35]. Reduction potential of the DHZ phenoxyl radical may be expected for an *ortho*-methoxy-substituted phenoxyl radical, indicating only moderate electron-donating ability. However, taking into account the literature data for anodic oxidation of compounds with 3-methoxy-4-hydroxyphenil subsistent in basic media, curcumin probably could be oxidized in the same manner. The Ni(II)-curcumin complex was shown in Fig. 2b. The mechanism of electrooxidation polymerization of the Nickel complexes is not clear at present.

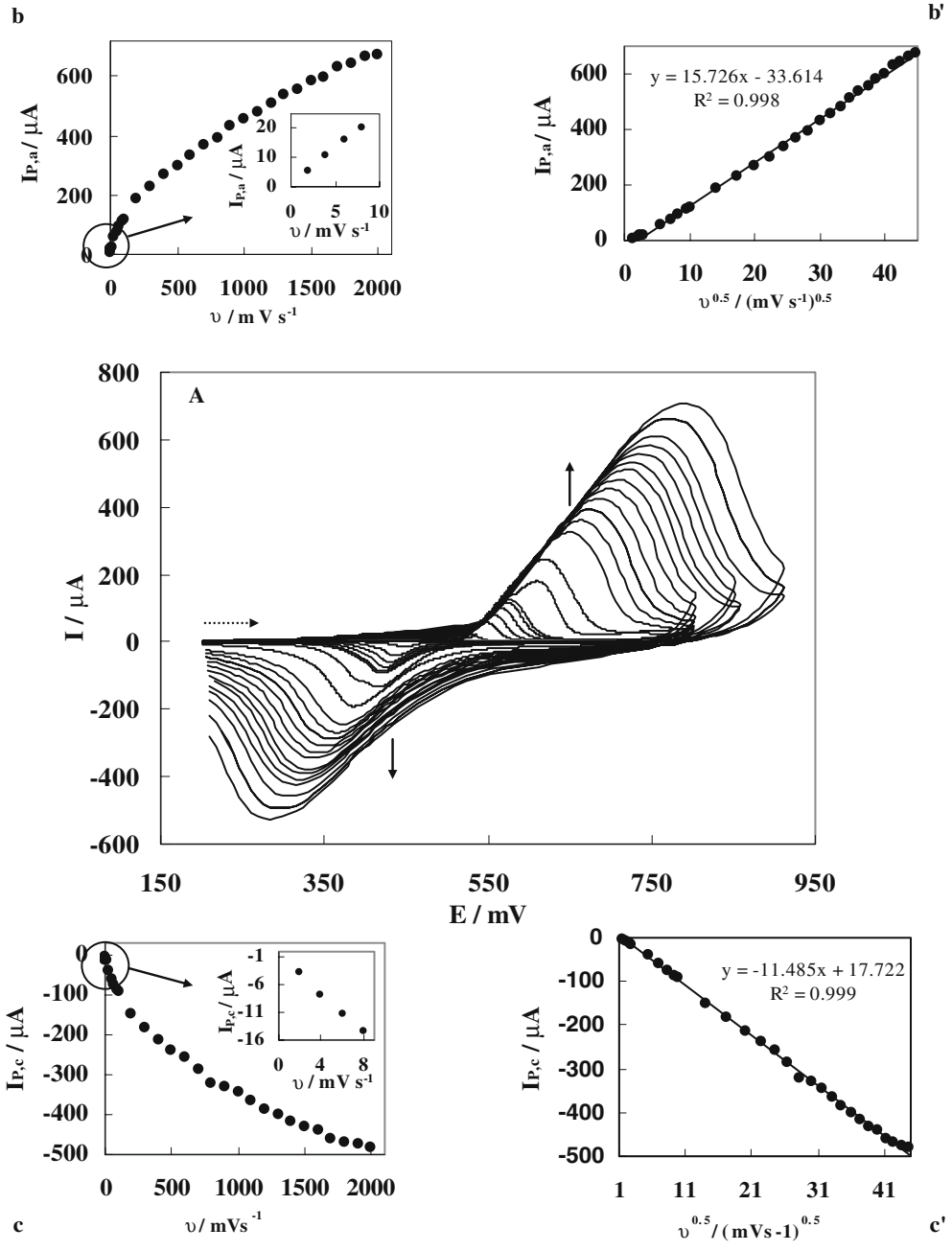

Fig. 3 **a** Typical cyclic voltammograms of a NCGC in 0.1 M NaOH at variety with the potential sweep rates of 2, 5, 10, 50, 70, 90, 100, 200, 300, 500, 600, 700, 800,1,000, 1,200, 1,300, 1,400, 1,500, 1,600, 1,700, 1,800, 1,900, and 2,000 mV s^{-1}. **b** and **c** The dependency of anodic and cathodic peak currents to the potential sweep rate. **b′** and **c′** Proportionality of anodic and cathodic peak currents to the square root of potential sweep rate

However, the mechanism of film formation is probably the same as for free curcumin, except that the presence of nickel in its structure makes it conductive and is responsible for the build up into the multiplayer system. Roslonek and Taraszewska [28] have proposed a tentative explanation for the electrochemical polymerization process by suggesting that the attachment of the nickel complexes to the electrode surface is connected to oxidation of OH^- anions. Indeed, a pH value of 13 is critical for film formation and one would expect that the oxidation of OH^- would create a variety of functional groups on the electrode surface. It is important to note that no electropolymerization processes occurred when the potential scan was limited to a range before the beginning of the oxidation of OH^-. Thus, coupling the complexes to the electrode surface via an −O-Ni(II) bond seems probable. During further scans, the attached nickel (II) complexes undergo oxidation to nickel (III) and bind to incoming nickel species, supplied to the electrode surface by diffusion, via oxo-bridges.

From cyclic voltammograms recorded at different potential sweep rates for curcumin solution, a linear change for the oxidation current peak in the first cycle with respect to the corresponding potential sweep rate was observed (data are not shown). Because the oxidation process of curcumin is observed only in the first cycle of potential, it can also be concluded that curcumin is oxidized. Oxidation products adsorbed on the surface forms a thin film, which is poorly defined as indicated by Cizewski et al. [9, 31, 36] probably proposed for oxidative of various compounds such as eugenol [31] and vanillin [37]. It is that of fouling effect, which is observed during oxidation of phenolics [38]. The peak of the thin film disappears after the next scans and a revisable electrochemistry system with a redox couple is observed.

The peak currents of oxidation and reduction of Ni-curcumin immobilized on the surface are proportional to the potential sweep rate resulted form cyclic voltammograms recorded at different potential sweep rates in a wide range of 2 to 2,000 mV s^{-1} by using GC-modified electrode in 0.1 M NaOH solution shown in Fig. 3. The inset of

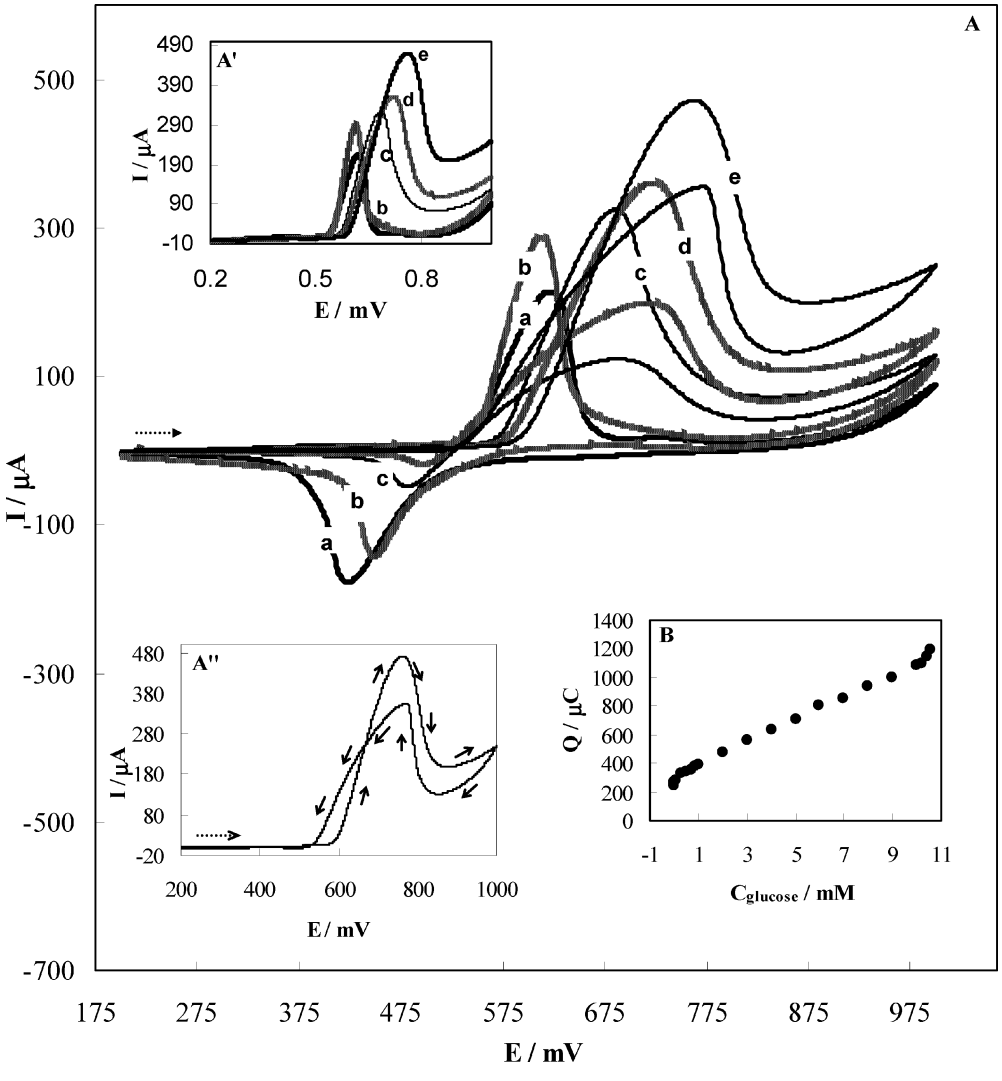

Fig. 4 **a** Cyclic voltammograms of the NCGC electrode in 0.1 M NaOH in the presence of various concentration of glucose: *a* 0; *b* 0.07; *c* 0.6; *d* 4; *e* 10 mM. The potential sweep rate was 100 mV s^{-1}. **a′** Similar to **a** otherwise the reveres sweep for better comparison were omitted. **a″** Typical cyclic voltammogram of the NCGC electrode in the presence of 10 mM glucose. **b** Plot of charge under the anodic peak during forward sweep vs various concentration of glucose in solution

Fig. 3b,c, respectively, shows that anodic and cathodic peak currents are directly proportional to the scan rate of potential at sweep rate below 10 mV s^{-1}. The linear relation between the peak currents and potential sweep rate confirms that the redox transition in Fig. 1, inset, is a surface process. However, at relatively high potential sweep rates (>10 mV s^{-1}) the dependency of peak currents is on the square root of potential sweep rate, as depicted in Fig. 3b′,c′. This indicated, in fact, the occurrence of a diffusion process as the rate limiting step in the total redox transition of modified film which may be related to the relative diffusion of counter ions (alkaline metal cations). This limiting diffusion process which is also reported for other Ni-modified electrodes [39, 40] may be occurred for the charge neutralization of the film during oxidation/reduction process.

The apparent total surface coverage Γ of the polyNCGC film electrode was calculated from the cyclic voltammograms of these film, the calculation being based on the charge under the Ni(II)-Ni(III) oxidative peak. The total surface coverage could be evaluated according to the following equation:

$$\Gamma = \mathrm{Q}/\mathrm{nFA} \tag{1}$$

The value of surface coverage for NCGC was 2.04×10^{-8} mol cm^{-2} that corresponds to the presence of multilayer of surface species. Γ increases with the number of electropolymerization potential scans. The potential of the redox couple and peak separation depends on the condition of film formation. Thin polyNCGC films formed after 20 scan ΔE is 114 mV and for thicker film, the peak separation increases, for example, after 80 scan peak separations is 285 mV at 100 mV s^{-1}.

Another point observed in Fig. 3a is that the peak-to-peak separation even at slow potential sweep rates has a finite value (e.g., 93 mV at 10 mV s^{-1}). This deviation of the redox process from the ideal surface redox process, appearing even at low scan rates may be attributed to the limitations associated with charge propagation in the film, the chemical interaction between the ions and the modifier film, the polarizability of the ions influencing its penetration in or out of the film, or nonequivalent sites in the film. At higher scan rates, a wider splitting appears indicating the limitation arising from the charge transfer kinetics [41].

Figure 4a shows cyclic voltammograms of the NCGC in 0.1 M NaOH in the absence (curve a) and presence of various concentrations of glucose (curves b–e) in the potential range of 200 to 1,000 mV by using a potential sweep rate of 100 mV s^{-1}. At the modified electrode, oxidation of glucose give rise to a typical electrocatalytic response, with an anodic peak current that greatly enhance over which observed for the modified surface in the absence of glucose and following by decreasing the cathodic current upon increasing the concentration of glucose in solution. In the presence of 1 mM glucose, the anodic peak enlarged, while its corresponding cathodic peak current diminished and the anodic charge associated with the anodic peak is quantitatively 72% more than that of the corresponding cathodic peak. In the contrary, in the absence of glucose, this is 19.2%. Charge is obtained by integrating the anodic and cathodic peaks under the background correction. Moreover, in the presence of glucose, the onset potential of the Ni(II) oxidation moiety shifted to positive value and enhances upon increasing the concentration of glucose. In fact, this indicated a strong interaction of glucose with the surface already covered by low valance nickel species. So, catalytic electrooxidation of glucose on NCGC seems to be certain. The anodic charge associated to the oxidation of low valance nickel species is proportional to the bulk concentration of glucose and any increase in the concentration of glucose causes an almost proportional linear enhancement of the anodic charge (Fig. 4b). This proportionality is linear in the range of 1 μM and 10 mM $\left(\mathrm{Q} = 77.816\mathrm{C}_{\mathrm{glucose}} + 313.320,\ \mathrm{R}^2 = 0.998,\ \mathrm{n} = 20\right)$. In addition, an anodic peak in the beginning of cathodic half cycle appeared. The appearance of an anodic peak in the anodic as well as in the reverse sweep is the distinct feature of electrocatalytic oxidation of hydroxy-containing compounds (e.g., small alcohols) on noble metals [42].

On the basis of the reported data and a literature review [20], the following mechanism is proposed for the mediated oxidation of glucose on the modified surface. The redox transition of nickel species is

$$\mathrm{Ni(II)} \Leftrightarrow \mathrm{Ni(III)} + \mathrm{e} \tag{2}$$

which the rate constants k_1 and k_{-1} are obviously potential dependent according to the following equation:

$$\mathrm{k}_1 = \mathrm{k}^\circ \exp\left[-\alpha \mathrm{nF}\eta/\mathrm{RT}\right] \tag{3}$$

$$\mathrm{k}_{-1} = \mathrm{k}^\circ \exp\left((1-\alpha)\mathrm{nF}\eta/\mathrm{RT}\right) \tag{4}$$

and glucose is oxidized on modified surface via the following reaction:

$$\mathrm{Ni(III)} - \text{curcumin} + \text{Glucose} \xrightarrow{\mathrm{k}_2} \text{Intermediate} + \mathrm{Ni(II)} - \text{curcumin} \tag{5}$$

Through the final electron transfer process, where the intermediate is further oxidized to the products, gluconic acid was produced. As reported in the literature [22–43], gluconolactone (or gluconate) and gluconic acid were detected as the main products of oxidation of glucose. In addition, formate and oxalate were detected as oxidation products of glucose [44].

$$\mathrm{Ni(III)} - \text{curcumin} + \text{Intermediate} \xrightarrow{\mathrm{k}_3} \text{Product} + \mathrm{Ni(II)} - \text{curcumin} \tag{6}$$

The electrocatalytic oxidation of glucose occurs not only in the anodic but also continues in the initial stage of the cathodic half cycle. Glucose molecules adsorbed on the Ni (II) species are oxidized at higher potentials parallel to the oxidation of Ni(II)-curcumin to Ni(III)-curcumin species. The later process has the consequence of decreasing the number of sites for glucose adsorption that along with the poisoning effect of the products or intermediates of the reaction tends to decrease the overall rate of glucose oxidation. Thus, the anodic current passes through a maximum as the potential is anodically swept. In the reverse half cycle, the oxidation continues and its corresponding current goes through the maximum due to the regeneration of Ni(II)-curcumin species that are active sites for the adsorption of glucose. Surely, the rate of glucose oxidation as signified by the anodic current in the cathodic half cycle drops as the unfavorable cathodic potentials are approached. Also, continuous cyclic voltammograms of NCGC in the presence of glucose showed that glucose reacted with the surface and no poisoning effect on the surface was observed.

Cyclic voltammograms of NCGC in the presence of 1 mM glucose at various potential sweep rates and the proportionality of anodic peak currents to the square root of sweep rates in a range of 2 to 2,000 mV s^{-1} illustrated in Fig. 5a,b, respectively. The cathodic peaks were not observed in the low scan rates, but appeared with increasing sweep rates up to 300 mV s^{-1}. Meanwhile, the anodic peak currents are linearly proportional to the square root of scan rate (Fig. 5b), suggesting that the overall oxidation of glucose at this electrode might be controlled by diffusion of glucose from solution to the redox sites on the surface. Moreover, a plot of the scan rate-normalized current ($I/v^{1/2}$) with respect to scan rate (Fig. 5c) exhibited a typical shape of an electrochemical–chemical (EC′) catalytic process [45].

Shown in Fig. 6a is a steady-state *I–E* curve, which for electrocatalytic oxidation of glucose recorded after 20 s, polarization at desired potential. A typical s-shape plot has been obtained and the transfer coefficient (α) can be found by plotting *E* vs log *I*. The slope of this plot is equal to 2.3RT/αF, which is obtained as 0.146 mV decade. So the charge transfer coefficient obtained is α=0.59.

Setting the working electrode potentials to desired values, the measurement of the catalytic rate constant as well as the diffusion coefficient of glucose was performed Choronoamperometric measurements of glucose at NCGC. Figure 7a shows double steps choronoamperograms for the NCGC in the absence (a) and presence (b–f) of glucose over a concentration range of 1 μM to 10 mM with an applied potential steps of 700 and 300 mV, respectively. Plotting of net current with respect to the mines square roots of time, which has been obtained by removing the background current, presents a linear dependency. The dominance of a diffusion-controlled process is pointed out. By using the slope of this line and according to Cottrell equation, the diffusion coefficient of glucose can be obtained [46]:

$$I = nFAD^{1/2}C\pi^{-1/2}t^{-1/2} \quad (7)$$

where *D* is diffusion coefficient and *C* is the concentration in mol cm^{-3}. The mean value of the diffusion coefficient of glucose was found to be 6.70×10^{-6} cm^2 s^{-1}, which is in good agreement with value reported in the literature [47]. The current is also neglible when potential is stepped down to 350 mV, indicating the irreversibility of glucose oxidation process.

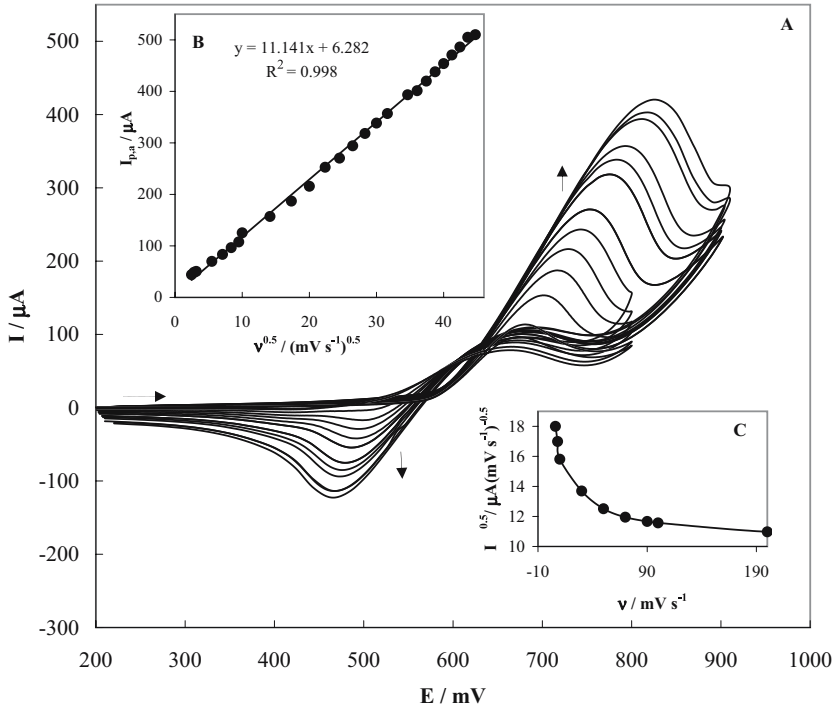

Fig. 5 **a** Typical cyclic voltammograms of the NCGC in 0.1 M NaOH in the presence of 1 mM glucose at various potential sweep rates of 2, 5, 10, 30, 50, 70, 80,100, 200, 300, and 400 mV s^{-1}. **b** Dependence of anodic peak current during the forward sweep on the square roots of sweep rate. **c** The anodic current function ($I/v^{1/2}$) vs potential sweep rate

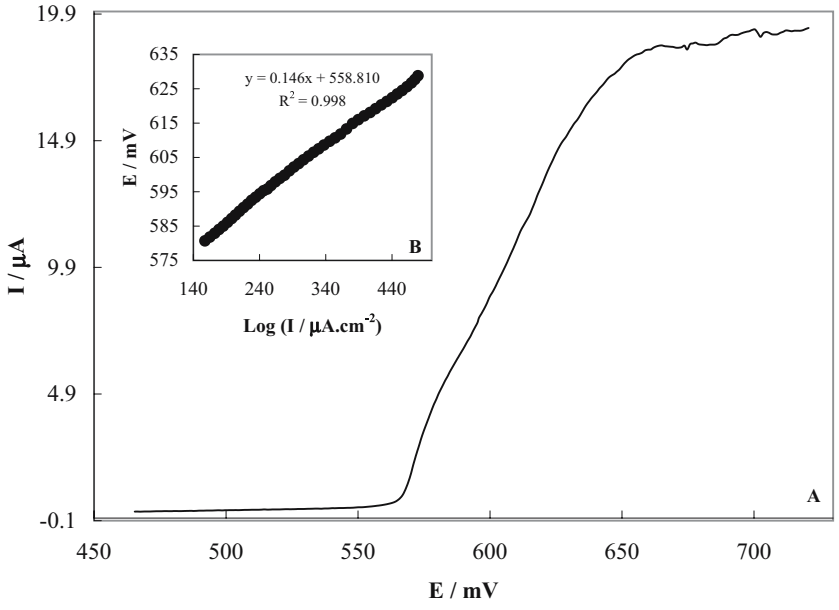

Fig. 6 **a** Potentiodynamic polarization curve for NCGC electrode in 0.1 M NaOH in the presence of 1 mM recorded using a potential sweep rate of 0.005 mV s^{-1}. **b** Tafel plot for NCGC electrode in 0.1 M NaOH in the presence of 1 mM glucose

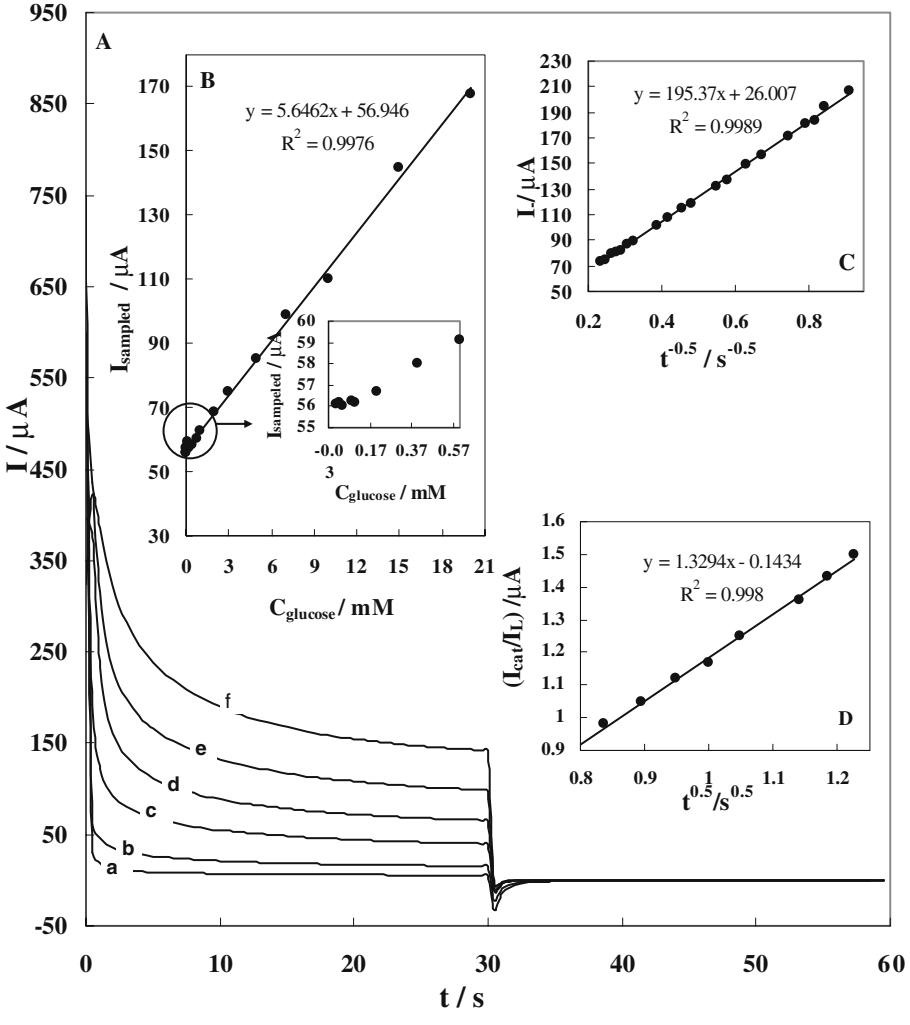

Fig. 7 **a** Chronoamperograms recorded for the NCGC electrode in 0.1 M NaOH solution in the absence *a* and presence of glucose *b–f* of various concentration of glucose: 0.01, 0.2, 0.8, 3, and 10 mM. The potential steps were 700 and 350 mV , respectively. **b** Plot of sampled transient current at fixed time of 10 s vs glucose concentration in the range of 1 μM to 20 mM. **c** Dependency of transient current on $t^{-0.5}$. **d** Dependency of I_{cat}/ I_L on the $t^{1/2}$ derived from the chronoamperograms represented in part **a**

Table 1 Some modified electrode used in electrooxidation of glucose

Substrate	Modifier	LOD	References
Glassy carbon electrode	Copper/copper oxide particles dispersed into a nafion film	0.5 μM	[50]
Glassy carbon electrode	Copper particles dispersed in to a polyanilin film	0.5 μM	[51]
Glassy carbon electrode	Carbon nanotube	10 μM	[52]
Graphit-like carbon film electrode	Nickel nanoparticles	20 nM	[53]
Glassy carbon and gold electrode	tetraruthenated Ni-porphyrin	0.36 μM	[22]
1-naphtylamine modified carbon paste electrode	Nickel particles dispersed into a poly(1-naphtylamine) film	6 μM	[20]

The number of electrons involved in the overall reaction can also be obtained from the dependency of anodic peak current on the square root of potential sweep rate (Fig. 5) according to the following equation for a totally irreversible diffusion controlled processes [48]:

$$I_p = 2.99 \times 10^5 n(\alpha)^{1/2} A D^{1/2} C \nu^{1/2} \quad (8)$$

where D is the diffusion coefficient of the glucose, obtained as 6.70×10^{-6} cm^2 s^{-1} form choroamperometric measurements, A is the electrode surface area, ν is the scan rate, I_P is the anodic peak current and C is the concentration of glucose. The number of electrons involved in the anodic oxidation of glucose obtained n=11.7.

Figure 7b shows the plot of sampled current at fixed time (10 s) with respect to the concentration of glucose in the range of 1 μM to 10 mM. A good linearity has been observed and a limit of detection of 0.1 μM has been obtained from three times the standard deviation of the blank per the slope of calibration curve [49]. These analytical parameters are compared to the results previously reported for electroanalytical determination of glucose with different sensors (see Table 1).

Choronoamperometry can also be used for the evaluation of the catalytic rate constant according to Pariente et al. [54]

$$I_{cat}/I_L = \gamma^{1/2}\left[\pi^{1/2}\mathrm{erf}\left(\gamma^{1/2}\right) + \mathrm{erf}(-\gamma)/\gamma^{1/2}\right] \quad (9)$$

where I_{cat} and I_L are the currents of the NCGC in the presence and absence of glucose and γ=kCt is the argument of the error function. k is catalytic rate constant, C is bulk concentration of glucose and t is elapsed time (s). In the cases where γ>1.5, erf($\gamma^{1/2}$) is almost equal to unity and the above equation can be reduced to:

$$I_{cat}/I_L = \gamma^{1/2}\pi^{1/2} = \pi^{1/2}(\mathrm{kCot})^{1/2} \quad (10)$$

From the slope of the I_{cat}/I_L vs $t^{1/2}$ plot, presented in Fig. 7d, the mean value of k for the concentration range of 1 μM to 10 mM of glucose was obtained as 6.50×10^3 M^{-1} s^{-1}.

Conclusion

The Ni-curcumin film was formed electrochemically in a regime of cyclic voltammetry on a glassy carbon electrode for electrooxidation of glucose in alkaline media. The modified electrode shows electrocatalytic oxidation of glucose at around 700 mV vs Ag/AgCl, while the glassy carbon electrode presents no activity. The oxidation process at more positive potential than the electrooxidation of redox couple Ni(II)/Ni(III) occurs. Using cyclic voltammetry and choronoamperometry techniques, the kinetic parameters such as charge transfer coefficient (α), the catalytic reaction rate constant (k), and the diffusion coefficient of glucose in the bulk of solution were determined. Moreover, the Ni-curcumin modified glassy carbon electrode exhibits large response current for oxidation of glucose.

Acknowledgements The authors gratefully acknowledge the support of Tarbiat Modarres University Research Council and the helpful discussions of Professor Golabi.

References

1. Zhang L, Dong S (2004) J Electroanal Chem 568:189
2. Golabi SM, Nourmohmmadi F, Saadnia A (2003) J Electroanal Chem 548:41
3. Pournaghi-Azar MH, Razmi-Nerbin H (1998) J Electroanal Chem 456:83
4. Liang J, Kucernak A (2003) J Electroanal Chem 543:187
5. Deronzier A, Moutet JC (1996) Coord Chem Rev 147:339
6. Xu F, Li H, Cross SJ, Guarr TF (1994) J Electroanal Chem 368:221
7. Cataldi TRI, Centonze D, Ricciardi G (1995) Electroanalysis 7:312
8. Ciszewski A, Milczarek G (1996) J Electroanal Chem 413:137
9. Ciszewski A, Milczarek G, Lewandowska B, Krutowski K (2003) Electroanalysis 15:518
10. Reim RE, Van Effen RM (1986) Anal Chem 58:3203
11. Casella IG, Gatta M (2000) Anal Chem 72:2969
12. Sung WJ, Bae YH (2000) Anal Chem 72:2177
13. De Mele MFL, Videla HA, Arvia AJ (1983) Bioelectrochem Bioenerg 10:239
14. Luo MZ, Baldwin RP (1995) J Electroanal Chem 387:87
15. Matsumoto F, Harada M, Koura N, Uesugi S (2003) Electrochem Commun 5:42
16. Wang J, Taha Z (1990) Anal Chem 62:1413
17. Reim RE, Van Effen RM (1986) Anal Chem 58:3203

18. Santos LM, Baldwin RP (1987) Anal Chem 59:1766
19. Vassilyev YuB, Khazova OA, Nilolaeva NN (1985) J Electroanal Chem 196:127
20. Ojani R, Raoof JB, Salmany-Afagh P (2004) J Electroanal Chem 571:1
21. Warren S, McCormac T, Dempsey E (2005) Bioelectrochemistry 67:23
22. Araki K, Eisi Toma H, Angnes L (2005) Anal Chim Acta 539:215
23. Mousavi MF, Rahmani A, Golabi SM, Shamsipur M, Sharghi H (2001) Talanta 55:305
24. Arvand M, Mousavi MF, Zanjanchi M, Shamsipur M (2003) J Pharm Biomed 33:975
25. Trevin S, Bedioui F, Devynck J (1996) J Electroanal Chem 408:261
26. Vilas-Boas M, Freire C, de Castro B, Hillman AR (1998) J Phys Chem B 102:8533
27. Trevin S, Bedioui F, Guadalupe Gomez Villegas M, Bied-Charreton C (1997) J Mater Chem 7:923
28. Roslonek G, Taraszewska J (1992) J Electroanal Chem 325:285
29. Wang YJ, Pan MH, Cheng AL, Lin LI, Ho YS, Hsieh CY, Lin JK (1997) J Pharm Biomed Anal 15:1867
30. Masuda T, Toi Y, Bando H, Maekawa T, Takeda Y, Yamaguchi H (2001) J Agric Food Chem 50:2524
31. Ciszewski A, Milczarek G (1999) Anal Chem 71:1055
32. Mac Tylor CE, Ewing AG (1997) Electroanalysis 9:755
33. Buchi G, Mak CP (1977) J Am Chem Soc 99:8073
34. Unda C, Tse CSD, Kuwana T (1982) Anal Chem 54:850
35. Jovanovic SV, Steenken S, Boone CW, Simic MG (1999) J Am Chem Soc 121:9677
36. Ciszewski A (1995) Electroanalysis 7:1132
37. Vexmillion FJ, Pearl IA (1964) J Electrochem Soc 111:1392
38. Ureta-Zanartu MS, Mora ML, Diez MC, Berrios C, Ojeda J, Gutierrez C (2002) J Appl Electrochem 32:1211
39. Jafarian M, Mahjani MG, Heli H, Gobal F, Heydarpoor M (2003) Electrochem Commun 5:184
40. Salimi A, Abdi K, Khayatiyan R (2004) Electrochemica Acta 49:413
41. Pournaghi-Azar MH, Dastangoo H (2004) J Electroanal Chem 573:355
42. Becer_Ik I, Kadirgan F (2001) Turk J Chem 25:373
43. Tominaga M, Shimazoe T, Nagashima M, Taniguchi I (2005) Electrochem Commun 7:189
44. Farrell ST, Breslin CB (2004) Electrochimica Acta 49:4497
45. Nicholson RS, Shain I (1964) Anal Chem 36:706
46. Bard AJ, Faulkner LR (2001) Electrochemical methods, fundamentals and applications. In: Bard AJ (ed) Chap. 5. Wiley, New York, p 209
47. Torto N, Ruzgas T, Gorton L (1999) J Electroanal Chem 464:252
48. Bard AJ, Faulkner LR (2001) Electrochemical methods, fundamentals and applications. In: Bard AJ (ed) Chap. 6. Wiley, New York, p 236
49. Ingel JD, Crouch SR (1988) Spetrochemical Analysis. In: Prentice-Hall, Inc, p 173
50. Eramo FD, Marioli JM, Arevalo AA, Sereno LE (1999) Electroanalysis 11:481
51. Casella IG, Cataldi TRI, Guerrieri A, Desimoni E (1996) Anal Chim Acta 335:217
52. Deo RP, Wang J (2004) Electrochem Commun 6:284
53. You T, Niwa O, Chen Z, Hayashi K, Tomita M, Hirono S (2003) Anal Chem 75:5191
54. Pariente F, Lorenzo E, Tobalina F, Abruna HD (1995) Anal Chem 67:3936